Inst. Phys. Conf. Ser. No 153: Section 3
Paper presented at Electron Microscopy and Analysis Group Conf. EMAG97, Cambridge, 1997

© 1997 IOP Publishing Ltd

The determination of the ionicity of sapphire using energy-filtered high resolution electron microscopy

S J Lloyd, R E Dunin-Borkowski† and C B Boothroyd

Department of Materials Science and Metallurgy, Pembroke Street, Cambridge CB2 3QZ, UK
† Center for Solid State Science, Arizona State University, Tempe, AZ 85287-1704, USA

ABSTRACT: The sensitivity of high resolution images to the degree of ionicity of sapphire is assessed through a comparison of experimental [$2\bar{1}\bar{1}0$] images with simulations. It is shown that, while the degree of ionicity does indeed affect image contrast, its quantification requires the determination of microscope imaging parameters to an unfortunately high degree of accuracy. Significantly, in contrast to previous results, the contrast of the experimental high resolution images is found to be *comparable* to that of the simulations. The reasons for this unusual lack of discrepancy are discussed, as are the potential advantages of electron holography rather than high resolution electron microscopy for determining the ionicities of such materials.

1. INTRODUCTION

The success of convergent beam electron diffraction (CBED) for measuring bonding charge densities in pure materials has resulted not only from the sensitivity of low order structure factors to the distribution of valence electrons (e.g. Midgley and Saunders, 1996) but also from the insensitivity of the fitting procedure to the magnitudes of certain microscope and specimen parameters whose determination plagues similar quantitative matching for high resolution images. However, alternative approaches to CBED that are better suited to the characterisation of charge transfer and bonding at interfaces, and which do not rely on the use of a focused probe that may damage beam-sensitive samples, are required. Accordingly, here we continue the investigations of Stobbs and Stobbs (1995) and Gemming et al. (1996) in an assessment of the sensitivity of high resolution images of [$2\bar{1}\bar{1}0$] sapphire (Al_2O_3) to ionicity and the importance of including ionic scattering factors in simulations. The suitability of sapphire for such an investigation results in part from its large unit cell, while in the [$2\bar{1}\bar{1}0$] orientation the amplitudes of certain beams that contribute to the image are sensitive to differences between the scattering factors of Al and O as opposed to their sums. The high resolution image simulations presented below were carried out using the tabulated X-ray scattering factors of Rez et al. (1994) and incorporated representative parameters for a JEOL 4000FX operating at 397kV (C_s=2mm, Δf=15nm, beam semi-angle 0.5mrad, objective aperture radius 20.6mrad). Debye-Waller factors for Al_2O_3 were taken from Kirfel and Eichhorn (1990).

2. RESULTS AND DISCUSSION

Fig.1 shows the sum of the electron scattering factors for Al and O for one formula unit of Al_2O_3, as calculated for neutral and fully ionic species from the tabulated X-ray scattering factors of Rez et al. (1994), while the amplitudes of the Fourier coefficients of the projected potential are plotted as a function of spatial frequency (with $s=\sin\theta/\lambda$) for both neutral and ionic scattering factors in fig.2. Similarities are apparent between figs. 1 and 2 in that the differences between the neutral and ionic calculations extend to ~5nm^{-1}. In fig.2, the difference is greatest for the spatial frequencies that depend on the difference between the scattering factors of Al and O (e.g. $01\bar{1}2$ and 0006) rather than on their sum (e.g. $03\bar{3}0$), the greatest fractional difference occurring for the 0006 beam (for which the sense of the change as a function of ionicity is opposite to that for $01\bar{1}4$ and $01\bar{1}2$).

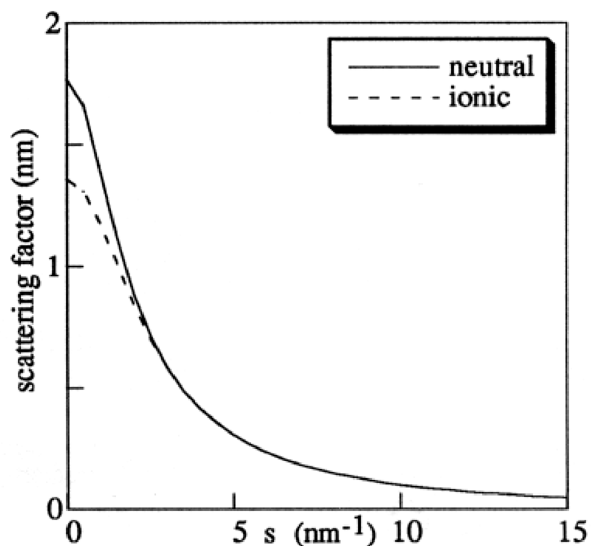

Fig.1 Electron scattering factors for one unit cell of Al_2O_3 determined using neutral and ionic scattering factors ($s=\sin\theta/\lambda$).

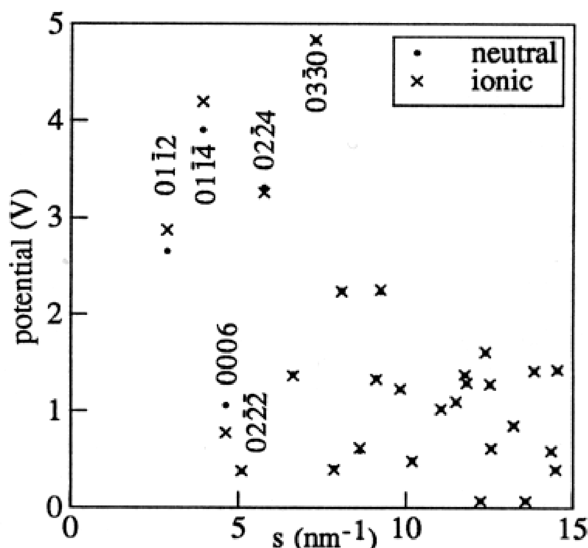

Fig.2 Fourier coefficients of projected potentials calculated using neutral and ionic scattering factors. (V_0=19.9 and 15.3V for neutral and ionic scattering factors respectively).

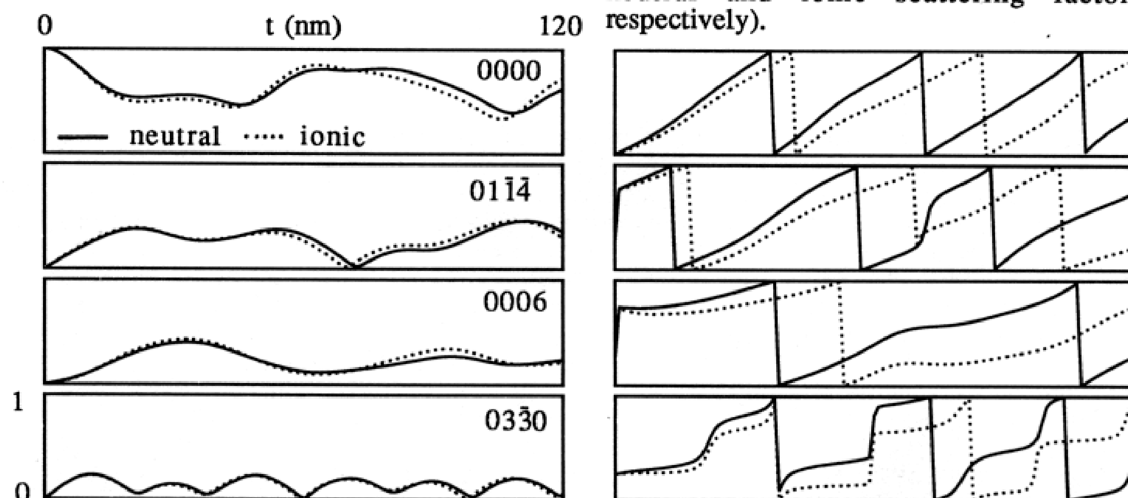

Fig.3 Amplitudes (left) and phases (right) of selected beams as a function of foil thickness (t).

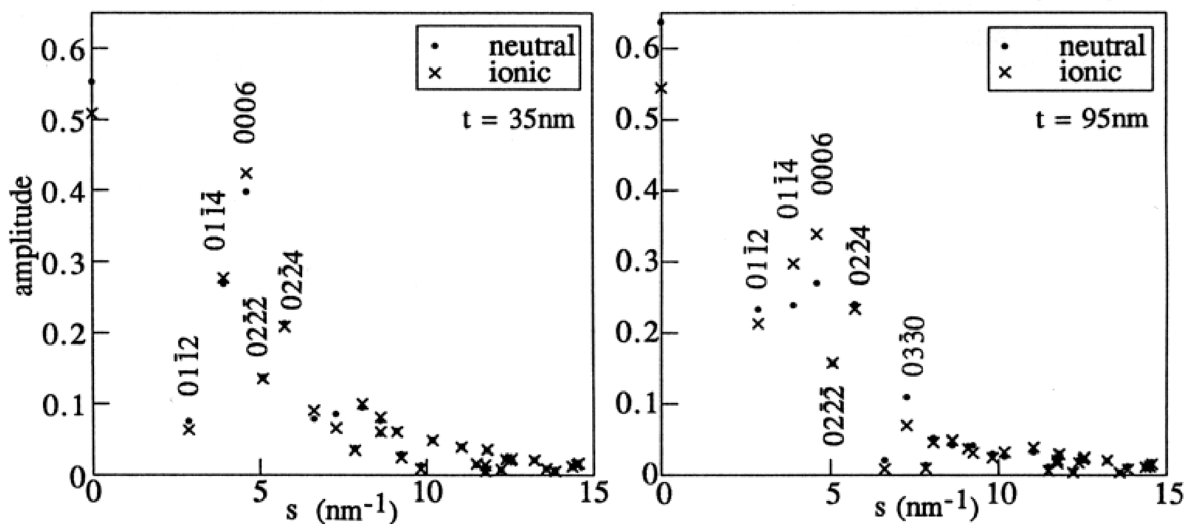

Fig.4 Fourier coefficients of image contrast as a function of s at foil thicknesses of 35 and 95nm.

Fig.3 shows the amplitudes and phases of selected beams plotted as a function of foil thickness. The fact that the effect of ionicity on the beam amplitudes increases with foil thickness as a result of dynamical diffraction can be seen clearly in fig.4, which shows beam amplitudes plotted as a function of s for two foil thicknesses. At the lower thickness of 35nm, the amplitudes follow the trends exhibited by the Fourier coefficients of potential in fig.2, with the exception of the 0006 and 03$\bar{3}$0 beams whose intensity is largely governed by double diffraction. (In fact, for 0006 the sense of the change in amplitude as a function of ionicity is reversed relative to fig.2). At the greater foil thickness of 95nm, dynamical effects are now dominant and the beam amplitudes are more sensitive to ionicity than at 35nm. (Stobbs and Stobbs (1995) found even greater differences in beam amplitudes as a function of ionicity for an accelerating voltage of 1200kV, although ionic scattering factors were included differently in their simulations.)

Fig.5 shows a comparison of energy-filtered experimental images (obtained with an energy window of 10eV centred on the zero-loss peak) and simulations for foil thicknesses of 35 and 95nm. The Al_2O_3 specimen was made by dimpling a disc of single crystalline sapphire that had a [2$\bar{1}\bar{1}$0] surface normal, ion-milling to perforation, removing organic and metallic contaminants by washing in aqua regia, and then annealing the sample for 8 hours at 1450°C to allow reconstruction of the surface (Tietz et al. 1992). The simulated images show that at 35nm the difference in the 0006 beam amplitude as a function of ionicity is not sufficient to result in significant image pattern changes. Although the image pattern is distinguishable between the simulations at a thickness of 95nm, particularly at a defocus of -96nm, the discrepancy between the experimental pattern and both sets of simulations is greater than that between the two simulations, as a result of the extreme sensitivity of the

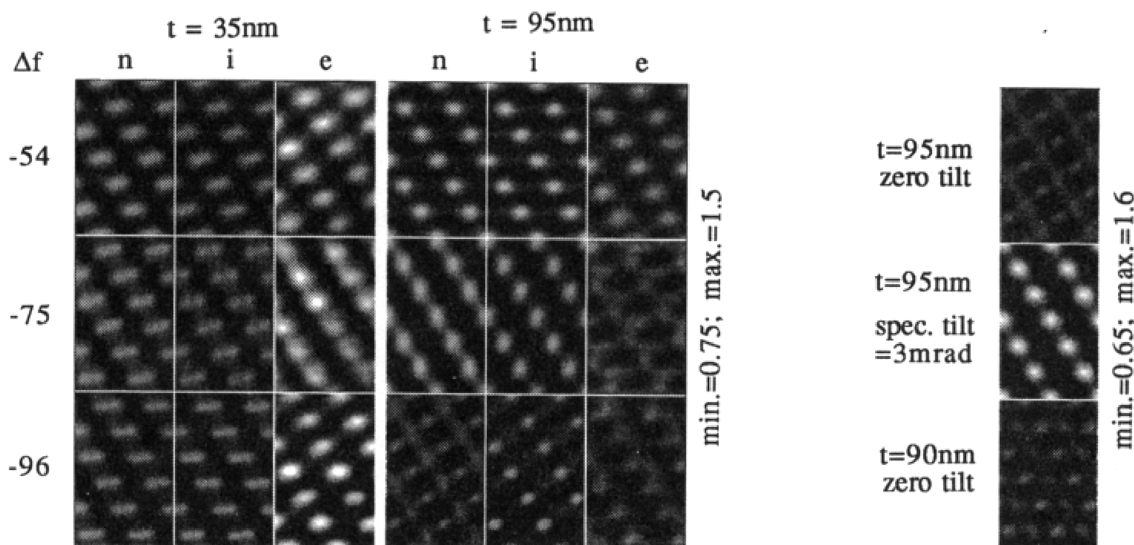

Fig.5 Images simulated using neutral (n) and ionic (i) scattering factors, as compared to experimental (e) data as a function of defocus (Δf) for two foil thicknesses.

Fig.7 Simulated images compared for different imaging conditions (Δf = -96nm)

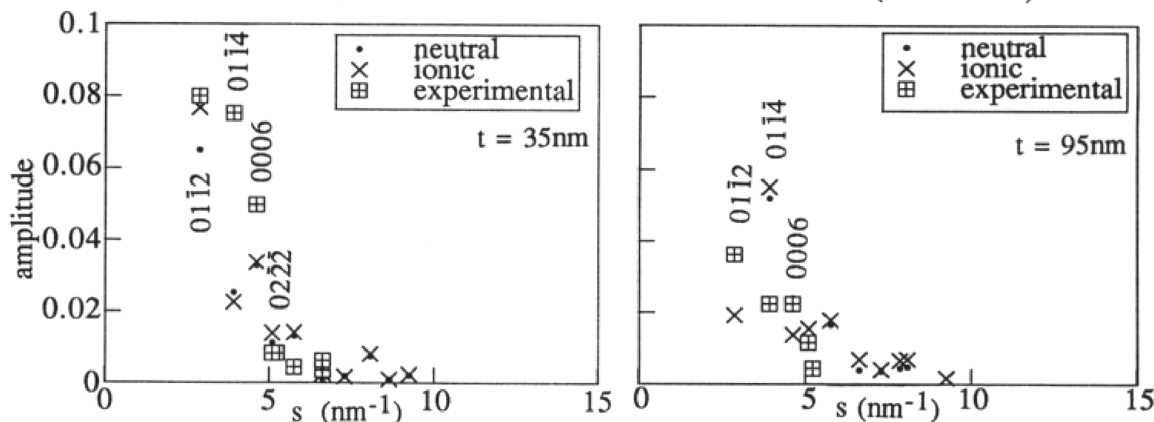

Fig.6 Fourier coefficients of experimental and simulated image contrast for foil thickness of 35nm and 95nm and a defocus of -96nm.

image pattern to the experimental imaging conditions. Fourier coefficients of the image contrast are plotted as a function of s in fig.6 for both the experimental and the simulated images for a foil thickness of 95nm and a defocus of -96nm. While the details of the variation in contrast with s are not reproduced by either set of simulated images, it is significant and unusual that the magnitude of the contrast in the experimental and simulated images is comparable (see Boothroyd, 1997). The sensitivity of the image pattern to the imaging conditions is a consequence of the strongly dynamical nature of the scattering. This is illustrated in fig.7, which shows the effect of a small change in specimen tilt and foil thickness on one of the simulated images. Paradoxically, it appears that the close match between the experimental and simulated image contrast results from the use of a clean specimen that has no amorphous surface layer, whereas this attribute makes the accurate determination of defocus and specimen tilt difficult. The solution may lie in the use of an experimental tilt series to determine the imaging parameters accurately (Saxton, 1995).

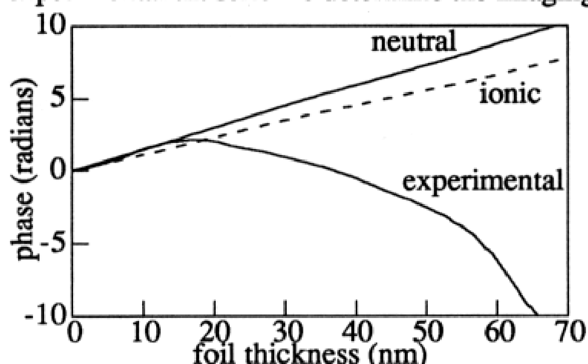

Fig.8 Experimental and simulated phase of holographic interference fringes as a function of thickness (see text for details).

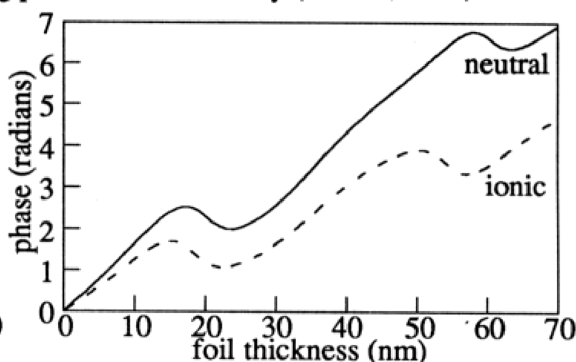

Fig.9 Simulated phase of holographic interference fringes at the [0001] zone axis,

It was clear from fig.3 that the phases of the beams show a strong dependence on ionicity - and there is a correspondingly large difference in the mean inner potential V_0 for Al_2O_3 of 23% between values calculated using neutral and ionic scattering factors. While neither high resolution imaging nor CBED can be used to determine V_0 for a pure material, we now discuss the use of electron holography to determine V_0 and hence ionicity. A preliminary experimental hologram of a sapphire sample with an [0001] foil normal was obtained using a Philips CM200 FEG operated at 200kV with a voltage of 100V applied to the biprism. The foil was tilted from the [0001] zone axis to a weakly diffracting orientation, and the resulting phase of the holographic fringes is shown in fig.8 as a function foil thickness, alongside full multislice simulations of the phase for the experimental conditions using both neutral and ionic scattering factors. The experimental phase profile is only consistent with the simulations in the thinnest regions of the foil, probably as a result of charging of the specimen due to its lack of carbon contamination. Both dynamical effects and absorption were included in the simulations and so cannot be responsible for this discrepancy. (Fig.9 shows that the simulated phase does not reverse in the manner observed experimentally even for a foil oriented exactly at the [0001] zone normal, at which dynamical effects should be strongest). However, the sensitivity of electron holographically-measured phase to ionicity at both weakly diffracting and more dynamical orientations, as well as the simplicity of such a measurement as compared with the quantitative analysis of high resolution image contrast, is beyond doubt.

We are grateful to Trinity Hall, Cambridge for financial support and to D J Smith and M R McCartney for the use of laboratory facilities at Arizona State University. We also thank A R Preston for help with the calculations and P A Midgley for useful discussions.

REFERENCES

Boothroyd CB 1997 J. Microscopy, in press
Gemming T, Exner M, Wilson M, Möbus G and Rühle M 1996 Presented at EUREM Dublin
Kirfel A and Eichhorn K 1990 Acta. Cryst. A46, 271
Midgley PA and Saunders M 1996 Contemp. Phys. 37, 441
Rez D, Rez P and Grant I 1994 Acta Cryst. A50, 481
Saxton WO 1995 J. Microscopy 179, 201
Stobbs S H and Stobbs W M 1995 Inst. Phys Conf Ser. 147, 83
Tietz L A, Summerfelt S R and Carter C B 1992 Phil. Mag. A 65, 439